

Unidirectional lasing from InGaN multiple-quantum-well spiral-shaped micropillars

G. D. Chern, H. E. Tureci, A. Douglas Stone, and R. K. Chang^{a)}
Department of Applied Physics, Yale University, New Haven, Connecticut 06520

M. Kneissl and N. M. Johnson
Palo Alto Research Center (PARC), Palo Alto, California 94304

(Received 21 January 2003; accepted 18 June 2003)

We report unidirectional emission from lasing in $\text{In}_{0.09}\text{Ga}_{0.91}\text{N}/\text{In}_{0.01}\text{Ga}_{0.99}\text{N}$ multiple-quantum-well spiral micropillars. Our imaging technique shows that the maximum emission comes from the notch of the spiral microcavities at an angle about 40° from the normal of the notch. At room temperature, the spiral microcavity lases near 400 nm when optically pumped with 266 or 355 nm light. A reduction in the lasing threshold and an improvement in unidirectionality occurs when the microcavity is selectively pumped near its boundary. © 2003 American Institute of Physics. [DOI: 10.1063/1.1605792]

A promising approach to making high- Q optical microresonators is to base them on totally internally reflected modes of dielectric microstructures. Such devices have received considerable attention as versatile elements for integrated optics and as low threshold semiconductor lasers. Initial work focused on whispering gallery mode (WGM) spherical,¹ cylindrical, and disk lasers.^{2–4} Some time ago,^{5–8} it was shown that smoothly deformed cylindrical lasers [asymmetric resonant cavities (ARCs)] could achieve highly directional emission and much improved output power. However, these microlasers (as well as those based on hexagonal,⁹ triangular,¹⁰ and square¹¹ cavities) were found to produce multiple output beams. In fact, it would seem that any lasing mode based on non-normal incidence rays (required for high- Q) would generate at least two output beams due to the possibility of interchanging incident and reflected rays.

In this letter, we report a design which provides unidirectional emission from an InGaN multiple-quantum-well (MQW) spiral-shaped microcavity laser. Theoretical work below indicates that the lasing mode is a non-emitting (counterclockwise rotating) WGM coupled out by diffraction at the notch of the spiral. Our design may be of great interest for future development of current-injection blue lasers.

The InGaN MQW heterostructures were grown by metalorganic chemical vapor deposition (MOCVD) on a c -plane [0001] oriented sapphire (Al_2O_3) substrate; the composition and dimensions are indicated in Fig. 1(a). The InGaN MQWs are sandwiched between two GaN layers, which are doped with Si and Mg to provide carriers for current injection of the microcavities in the future and allows for optical mode confinement along the axis of the cylinder due to the change in refractive index from the InGaN MQW layer to GaN layer. The Ga and In concentrations in the MQWs determine the output emission wavelength. Transverse modes of this structure have an effective index of refraction $n \approx 2.6$. The micro-

pillar samples were etched into spiral cross-sections, defined by

$$r(\phi) = r_0 \left(1 + \frac{\epsilon}{2\pi} \phi \right), \quad (1)$$

using chemically assisted ion beam etching (CAIBE) to a depth of about $1.5 \mu\text{m}$. Here, ϵ is the deformation parameter and r_0 is the radius of the spiral at $\phi=0$. The cross section jumps back to r_0 at $\phi=2\pi$ creating a “notch;” the unidirectional emission is from this notch [see, e.g., inset, Fig. 1(b)].

We optically excited the micropillars at room temperature using two different sources: a frequency tripled 355 nm or quadrupled 266 nm Nd:YAG Q -switched laser. A laser repetition rate of 1 Hz was used to avoid heating. The semiconductor sample was mounted on rotatable x - y - z translational stages and the pump beam was focused onto the

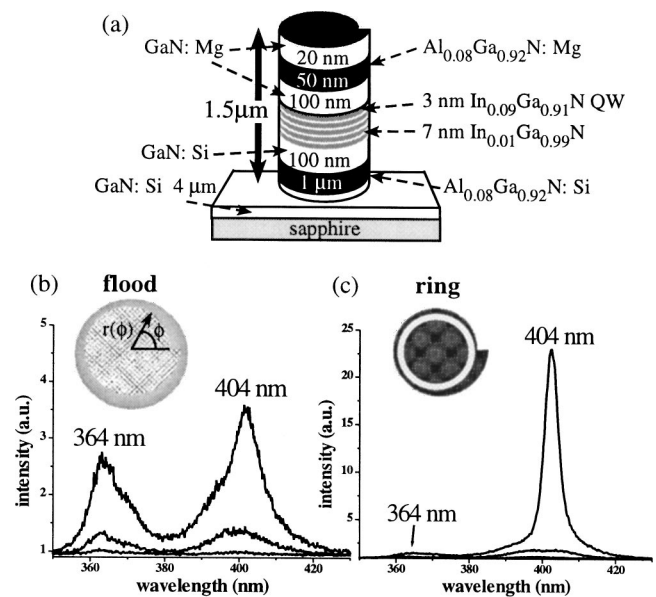


FIG. 1. (a) Structure of the InGaN MQW sample. Spectra of spiral microcavity ($\epsilon=0.10$ and $d=500 \mu\text{m}$) (b) flood-pumped and (c) ring-pumped with 266 nm light for increasing intensities. Peaks at 364 nm and 404 nm correspond to emission from GaN layers and InGaN MQWs, respectively.

^{a)}Electronic mail: richard.chang@yale.edu

sample at normal incidence to the top face of the micropillar. Light emission from the pillar sidewalls was imaged with a camera lens onto either a spectrometer for spectral analysis or an intensified charge coupled device (ICCD) for spatial imaging.

We focus here on the $d = r_0(2 + \frac{3}{2}\epsilon) = 500 \mu\text{m}$ pillars with $\epsilon = 0.10$, which had the lowest thresholds and narrowest emission lobes. Figure 1(b) shows the spectra obtained when the top face is uniformly exposed to the 266 nm pump (*flood pumping*). Spectra are shown for increasing pump intensities with strong emission peaks at 404 and 364 nm. The 404 nm emission is associated with localized exciton recombination in the InGaN MQW (active) layer. The 364 nm peak results from the band-gap recombination process in the GaN:Mg layers above the MQWs. As the input intensity increases, Fig. 1(b) shows that a narrow peak at 404 nm begins to appear, indicating the onset of amplified spontaneous emission (ASE).

Following Rex *et al.*,¹² we then selectively pumped the same cavity using an axicon lens to form a ring-shaped beam (*ring pumping*) to achieve better spatial overlap with the high- Q mode and thus lower the ASE and lasing threshold. The results are shown in Fig. 1(c). At the highest input power (2.17 kW), the 404 nm peak (with a spectrometer-limited width of 5 nm) for ring pumping is nearly an order of magnitude greater than that for flood pumping [full width at half maximum (FWHM) of 15 nm] and the ASE threshold was less than half that for flood pumping.

The 355 nm pump light was found to excite the InGaN MQWs more efficiently than 266 nm radiation. This is attributed to a smaller attenuation of the pump energy at 355 nm in the Mg-doped GaN layers. In fact, the absorption coefficient for GaN at 266 nm is $\alpha \sim 1.5 \times 10^5 \text{ cm}^{-1}$, about 1.5 times greater than that at 355 nm.¹³ Therefore, the intensity of 266 nm light reaching the MQWs is only half that of 355 nm light. We found that the peak wavelength from the MQW emission was blueshifted by as much as 10 nm when excited with 355 nm radiation.

When we ring pumped with 355 nm, at low pump intensities ($I_p < 500 \text{ kW/cm}^2$), we observed a region of slow growth ($I_o \sim I_p^{0.2 \pm 0.02}$) characteristic of spontaneous emission. Above $I_p = 500 \text{ kW/cm}^2$, the peak output intensity rapidly increased as $I_o \sim I_p^{2.8 \pm 0.1}$, clearly signaling the laser transition [see Fig. 2(a)].

Unidirectionality of this lasing emission is shown in the farfield image of Fig. 2(b). This polar plot is obtained by integrating over image profiles taken at 5° intervals of the camera angle θ_{ICCD} defined such that at $\theta_{\text{ICCD}} = 0^\circ$, detected emission is normal to the notch. Because we use this imaging technique, we can state definitely that the directional far-field lobe is from the notch [see inset, Fig. 2(b)].

The resonances (quasinormal modes) of the spiral-shaped dielectric resonator were calculated using a generalization of the scattering quantization¹⁴ approach, well suited for the short wavelength limit. These calculations show that there are indeed such dominantly notch-emitting quasibound states of the spiral microcavity and that these modes have high intensity near the perimeter, consistent with the ring-pumping results [see Fig. 3(a)]. However, these modes display a crucial difference from the regular WG modes of a

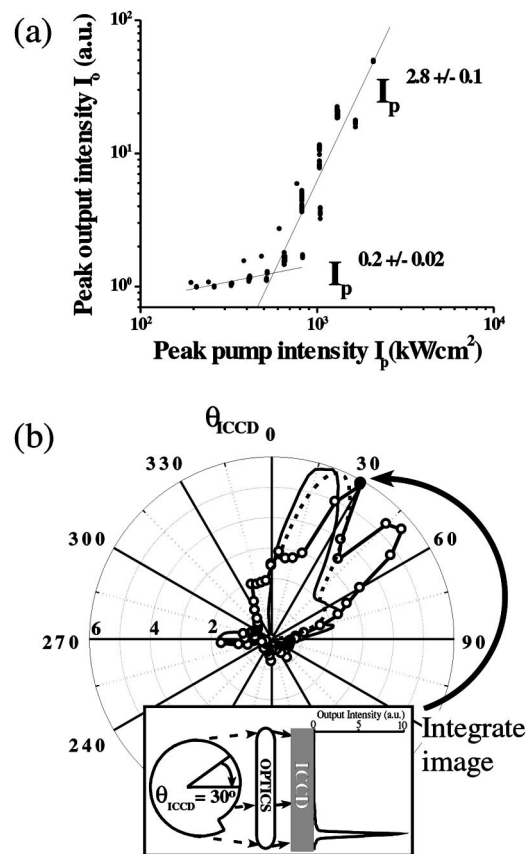


FIG. 2. (a) Log-log plot of peak output intensity I_o vs peak pump intensity I_p for ring pumping with 355 nm light; (b) unidirectional farfield emission pattern of the spiral. Experimental data (open circles) are in good agreement with the far-field pattern obtained from the numerical solution of the Helmholtz equation (solid line) and model calculations (dashed).

circular resonator: the high- Q resonances of the spiral exhibit a pronounced *chirality* and are predominantly composed of clockwise (cw) rotating components (corresponding to ray motion which could not escape at the notch). To illustrate this, we expand the electric field of the resonance in cylindrical harmonics:

$$E(\mathbf{r}) = \sum_{m=-\infty}^{+\infty} \alpha_m J_m(nkr) e^{im\phi}, \quad (2)$$

and plot the distribution of angular angular momentum components $|\alpha_m|^2$ in Fig. 3(b). In analogy with the cylindrical case we may interpret $m/nkR = \sin \chi$ as the sine of the average incidence angle of the rays on the boundary.⁶ The strong weighting of the distribution on negative components ($-m$) peaked around $|m| \approx 160$ corresponds to a mode with mostly cw-rotating waves having an angle of incidence $\sin \chi \approx 0.8$, which are hence totally internally reflected (the critical angle χ_c is defined by $\sin \chi_c = \pm 1/n = \pm 0.38$ for $n = 2.6$). The small amount of counterclockwise (ccw) rotating waves are responsible for emission at the notch and are due to diffraction of the cw-waves as they pass the inner corner of the notch [see Fig. 3(b)]. Various ray-tracing models fail to reproduce this behavior indicating that diffraction is crucial.

It is counterintuitive that the farfield emission lobe is not maximum at $\theta_{\text{ICCD}} = 0^\circ$ corresponding to normal emission from the notch, but is peaked at two angles: $\theta_{\text{ICCD}} \approx 30^\circ$ and

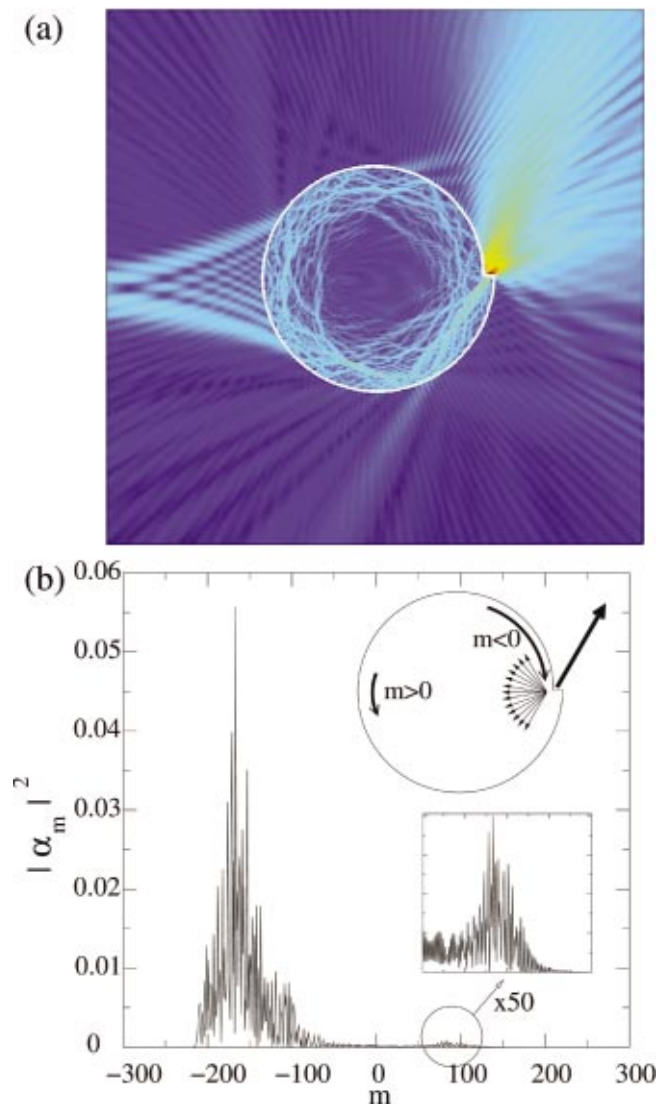


FIG. 3. (Color) (a) Real-space false color plot of the modulus of the electric field for a calculated quasibound state at $nkr_0 \approx 200$ at $\epsilon = 0.10$ deformation. (b) Distribution of angular momenta for the resonance plotted in (a). Note the peak at negative m , which corresponds to cw rotation and the small weight at positive m , which constitute the diffracted waves emitting from the notch.

$\theta_{\text{ICCD}} \approx 50^\circ$ [see Fig. 2(b)]. This tilt in the vicinity of the notch arises because the ccw component of the resonance is incident on the notch interface with a spread of wavevectors determined by the specific resonance. We can model this by an angular decomposition of the incident field on the notch

interface, which we assume to be composed of the $m < 0$ components only, and then propagating the emission into the farfield (this technique is described in Ref. 15). The calculated emission lobe(s), shown in Fig. 2(b), also has the deflection from $\theta_{\text{ICCD}} = 0^\circ$ and agrees fairly well with the farfield emission profile.

To summarize, we have demonstrated unidirectional lasing into free space by a dielectric microcavity, specifically a InGaN MQW spiral-shaped micropillar. This suggests an alternative design for future development of a class of current-injection blue lasers with features similar to vertical cavity surface emitting lasers (VCSELs) (e.g., that they can be arranged in two-dimensional arrays and devices can be tested on-chip), but without the materials challenges associated with the electrical and optical requirements for distributed Bragg reflector mirrors in a VCSEL structure.

The authors would like to thank T. Ben-Messaoud, S.-Y. Kuo, H. Schwefel, J. Wiersig, V. Boutou, D. W. Treat, N. Miyashita, and M. Teepe for their helpful contributions to this work. This work was partially supported by NSF, AFOSR, and the DARPA SUVOS program under SPAWAR Systems Center Contract No. N66001-02-C-8017.

- ¹S. X. Qian, J. B. Snow, H. M. Tzeng, and R. K. Chang, *Science* **231**, 486 (1986).
- ²S. L. McCall, A. F. J. Levi, R. E. Slusher, S. J. Pearton, and R. A. Logan, *Appl. Phys. Lett.* **60**, 289 (1992).
- ³S. M. K. Thiyagarajan, D. A. Cohen, A. F. J. Levi, S. Ryu, R. Li, and P. D. Dapkus, *Electron. Lett.* **35**, 1252 (1999).
- ⁴S. Anders, W. Schrenk, E. Gornik, and G. Strasser, *Appl. Phys. Lett.* **80**, 4094 (2002).
- ⁵J. U. Nöckel, A. D. Stone, G. Chen, H. L. Grossman, and R. K. Chang, *Opt. Lett.* **21**, 1609 (1996).
- ⁶J. U. Nöckel and A. D. Stone, *Nature (London)* **385**, 45 (1997).
- ⁷C. Gmachl, F. Capasso, E. E. Narimanov, J. U. Nöckel, A. D. Stone, J. Faist, D. L. Sivco, and A. Y. Cho, *Science* **280**, 1556 (1998).
- ⁸N. B. Rex, H. E. Tureci, H. G. L. Schwefel, R. K. Chang, and A. D. Stone, *Phys. Rev. Lett.* **88**, 094102 (2002).
- ⁹I. Braun, G. Ihlein, F. Laeri, J. U. Nöckel, G. Schulz-Ekloff, F. Schuth, U. Vietze, O. Weiss, and D. Wöhrle, *Appl. Phys. B: Lasers Opt.* **70**, 335 (2000).
- ¹⁰Y. Z. Huang, W. H. Guo, and Q. M. Wang, *Appl. Phys. Lett.* **77**, 3511 (2000).
- ¹¹A. W. Poon, F. Courvoisier, and R. K. Chang, *Opt. Lett.* **26**, 632 (2001).
- ¹²N. B. Rex, R. K. Chang, and L. J. Guido, *IEEE Photonics Technol. Lett.* **13**, 1 (2001).
- ¹³J. F. Muth, J. H. Lee, I. K. Shmagin, R. M. Kolbas, H. C. Casey, B. P. Keller, U. K. Mishra, and S. P. DenBaars, *Appl. Phys. Lett.* **71**, 2572 (1997).
- ¹⁴E. Doron and U. Smilansky, *Nonlinearity* **5**, 1055 (1992).
- ¹⁵H. E. Tureci and A. D. Stone, *Opt. Lett.* **27**, 7 (2002).